# CHAPTER-3

# Mononuclear Copper(II) Complexes with tetradentate pyrazole based ligand: Syntheses, Structures, DNA binding study and Antimicrobial activity

- **Paper published:**

  **Polyhedron 63 (2013) 147-155.**



Polyhedron 63 (2013) 147–155

Contents lists available at SciVerse ScienceDirect

Polyhedron

journal homepage: www.elsevier.com/locate/poly

## Mononuclear copper(II) complexes with a tetradentate pyrazole based ligand: Syntheses, structures, DNA binding study and antimicrobial activity

Ankita Solanki [a], Sujit Baran Kumar [a,*], Ankita A. Doshi [b], C. Ratna Prabha [b]

[a] Department of Chemistry, Faculty of Science, The Maharaja Sayajirao University of Baroda, Vadodara 390 002, India
[b] Department of Biochemistry, Faculty of Science, The Maharaja Sayajirao University of Baroda, Vadodara 390 002, India

**Abstract**

A series of mononuclear copper(II) complexes of the type [Cu(X)(dbdmp)]Y, where X = $N_3^-$, $NCS^-$, $NCO^-$, Y = $ClO_4^-$, $PF_6^-$ and $BF_4^-$ and dbdmp = *N*,*N*-diethyl-*N'*,*N'*-bis((3,5-dimethyl-*1H*-pyrazol-1-yl)methyl)ethane-1,2-diamine have been synthesized and characterized by microanalysis, physico-chemical and spectroscopic methods. Crystal structures of the four complexes $[Cu(N_3)(dbdmp)]ClO_4$ (**1**), $[Cu(NCS)(dbdmp)]ClO_4$ (**4**), $[Cu(NCS)(dbdmp)]PF_6$ (**5**) and $[Cu(NCO)(dbdmp)]ClO_4$ (**7**) were solved by single crystal X-ray diffraction studies and showed that all the complexes have distorted trigonal bipyramidal geometry. Interaction of CT-DNA with the complexes **1**-**6** were examined by spectroscopic titration and fluorescence techniques and showed the complexes have strong interaction with CT-DNA. Antimicrobial activity of the complexes (**1**-**6**) were studied by dilution method against *Gram positive* (*Bacillus subtilis)* and *Gram negative* (*Escherichia coli*) strain and showed the complete inhibition of the tested strains by the complexes.

## 3.1 Introduction

The synthesis, characterization and structure of transition metal complexes and their interaction with DNA have attracted much attention among the researchers as they have potential application in bioinorganic chemistry [1-6]. Transition metal complexes have been widely used for this purpose because of their flexible coordination behavior, different structural and electronic properties and bind with DNA by cleaving metal-ligand bond or by changing the coordination environment [7-8]. Although there are many reports on the interaction of DNA and transition metal complexes [9-22], the interaction of DNA and copper(II) complexes are very interesting because copper is an essential trace element bound to many proteins and enzymes [23-25]. There are many reports on CT-DNA binding study of copper(II) complexes with nitrogen containing ligands including polypyridine [26-27].

The interaction of DNA with transition metal complexes containing multidentate ligands is primary investigation to design a highly sensitive and appropriate diagnostic agent. The binding modes of complex with DNA are responsible for activity and the mechanism by which DNA replication is totally inhibited in cancer cells. Metal complexes generally bind to DNA via covalent and non-covalent interaction. In covalent binding, the labile ligand of the complexes interacts with a nitrogen base of DNA. The non-covalent DNA interactions modes are intercalation, electrostatic and groove binding of the cationic metal complexes along outside of DNA helix are of considerable interest. Most of the interaction of DNA with copper(II) complexes investigated so far the ligands are either bi- or tridentate nitrogen containing ligand. The investigation of DNA binding study of copper(II) complexes with pseudohalides and tetradentate $N_4$-coordinating pyrazole based ligand is scare.

In this chapter, we describe the syntheses and structural characterizations of mononuclear copper(II) complexes of the type [Cu(X)(dbdmp)]Y, where X = $N_3^-$ / $NCS^-$ / $NCO^-$, Y = $ClO_4^-$ / $PF_6^-$ / $BF_4^-$ and dbdmp = *N*,*N*-diethyl-*N'*,*N'*-bis((3,5-dimethyl-*1H*-pyrazol-1-yl)methyl)ethane-1,2-diamine. DNA binding study was performed using electronic absorption titrations and fluorescence quenching techniques. The antimicrobial activity of copper complexes against *Gram Positive* and *Gram negative* bacterial strains has been discussed in details.

## 3.2. Experimental

### 3.2.1. Materials

The chemicals and solvents were of analytical grade and purchased from commercial sources. Sodium azide, $Cu(CH_3COO)_2.H_2O$ (Qualigens, India), *N*,*N*-diethylethylenediamine, $NH_4PF_6$, $NH_4BF_4$ (Aldrich), CT-DNA, ethidium bromide, Tris(hydroxymethyl)aminomethane)hydrochloride (Tris-HCl) and NaCl (Spectrochem, India) were of reagent grade and used as received. $Cu(ClO_4)_2.6H_2O$ was prepared by reaction of copper carbonate with dilute $HClO_4$ acid and followed by slow evaporation of the solution.

### 3.2.2. Syntheses of Complexes

***Caution!*** Transition metal complex with perchlorate salt, azide ion and organic ligands are potentially explosive. Only a small amount of material should be synthesized and it should be handled with care.

#### 3.2.2.1. $[Cu(N_3)(dbdmp)]ClO_4$ (1)

To a stirring methanol solution (10 ml) of $Cu(ClO_4)_2.6H_2O$ (0.184 g, 0.5 mmol), ligand dbdmp (0.166 g, 0.5 mmol) in methanol (10 ml) was added and the colour changed immediately to deep blue. After 10 min, $NaN_3$ (0.033 g, 0.5 mmol) in minimum amount of water was added slowly to the mixture and the solution became dark green. This solution was stirred for 3h at room temperature, filtered and kept for slow evaporation. Green crystalline compound was obtained after five days, filtered and dried in vacuo. Yield. 0.240 g (89 %). Found C = 40.08, H = 6.05, N = 23.28 %. Anal calc for $C_{18}H_{32}N_9O_4ClCu$: C = 40.22, H = 6.01, N = 23.45 %. IR (KBr pellet) $cm^{-1}$; $\nu(N_3^-)$, 2054 vs; $\nu(C = C) + \nu (C = N)$/pz ring 1552 s, 1466 s; $\nu_{asmy}(Cl–O)$, 1106 br; $\delta(O–Cl–O)$, 623 s. UV-Vis spectra: $\lambda_{max}$/nm ($\varepsilon_{max}$/$mol^{-1}cm^{-1}$). 911 (70), 703 (108), 427 (830), 281 (1344). $\Lambda_M$ ($\Omega^{-1}cm^2\,mol^{-1}$) = 120. $\mu_{eff}$ = 1.76 BM.

#### 3.2.2.2. $[Cu(N_3)(dbdmp)]X$, X = $PF_6^-$(2), $BF_4^-$(3)

To a stirring solution of $Cu(CH_3COO)_2.H_2O$ (0.100 g, 0.5 mmol) in methanol (10 ml), ligand (0.166 g, 0.5 mmol) in methanol (10 ml) was added slowly and the colour changed to deep blue. After 10 min, $NaN_3$ (0.034 gm, 0.5 mmol) in water (1 ml) was added dropwise and the solution became dark green. Finally after 10 min,

$NH_4X$ (0.5 mmol) in water was added. This green solution was stirred for 4 h at room temperature, filtered and kept for slow evaporation. After 6 days green coloured crystalline compound was obtained which was washed with diethyl ether and dried in vacuo.

**[Cu($N_3$)(dbdmp)]$PF_6$** (**2**). Yield. 0.187 g (64 %). Found C = 37.21, H = 5.46, N = 21.59 %. Anal calc for $C_{18}H_{32}N_9PF_6Cu$: C = 37.08, H = 5.53, N = 21.62 %. IR (KBr pellet) $cm^{-1}$; ν($N_3^-$), 2049 vs; ν(C = C) + ν (C = N)/pz ring, 1557 s, 1466 s; ν($PF_6^-$), 843 br. UV-Vis spectra: $\lambda_{max}$/nm ($\varepsilon_{max}$/$mol^{-1}cm^{-1}$). 917 (85), 707 (137), 428 (935), 282 (1306). $\Lambda_M$ ($\Omega^{-1}cm^2\,mol^{-1}$) = 120. $\mu_{eff}$ = 1.76 BM.

**[Cu($N_3$)(dbdmp)]$BF_4$ (3)** Yield. 0.200 g (76 %). Found C = 41.15, H = 6.09, N = 24.45 %. Anal calc for $C_{18}H_{32}N_9BF_4Cu$: C = 41.19, H = 6.15, N = 24.02 %. IR (KBr pellet) $cm^{-1}$; ν($N_3^-$), 2053 vs; ν(C = C) + ν (C = N)/pz ring, 1554 s, 1467 s; ν($BF_4^-$), 1076 br. UV-Vis spectra: $\lambda_{max}$/nm ($\varepsilon_{max}$/$mol^{-1}cm^{-1}$). 920 (90), 707 (157), 429 (1108), 282 (1487). $\Lambda_M$ ($\Omega^{-1}cm^2mol^{-1}$) = 120. $\mu_{eff}$ = 1.76 BM.

### 3.2.2.3. [Cu(NCS)(dbdmp)]X, X = $ClO_4^-$ (4), $PF_6^-$ (5), $BF_4^-$(6)

The complexes were prepared by following the same procedure as for complex **1 - 3** except KSCN was used in the place of $NaN_3$. Green colored crystals were obtained after slow evaporation of solution.

**[Cu(NCS)(dbdmp)]$ClO_4$ (4).** Yield. 0.210 g (76 %). Found C = 41.13, H = 5.84, N = 17.85 %. Anal calc for $C_{19}H_{32}N_7O_4SClCu$: C = 41.22, H = 5.82, N = 17.71 %. IR (KBr Pellet) $cm^{-1}$; ν($NCS^-$), 2092 vs; ν(C = C) + ν (C = N)/pz ring, 1554 s, 1468 s; $\nu_{asmy}$(Cl–O), 1089 br; δ(O–Cl–O), 624 s. UV-Vis spectra: $\lambda_{max}$/nm ($\varepsilon_{max}$/$mol^{-1}cm^{-1}$). 896 (228), 727 (167), 411 (855), 271 (1154). $\Lambda_M$ ($\Omega^{-1}cm^2\,mol^{-1}$) = 120. $\mu_{eff}$ = 1.76 BM.

**[Cu(NCS)(dbdmp)]$PF_6$ (5).** Yield. 0.260 g (87 %). Found C = 37.91, H = 5.42, N = 16.49 %. Anal calc for $C_{19}H_{32}N_7OPF_6Cu$: C = 38.09, H = 5.38, N = 16.37 %. IR (KBr pellet) $cm^{-1}$; ν($NCS^-$), 2093 vs; ν(C = C) + ν (C = N)/pz ring, 1553 s, 1468 s; ν($PF_6^-$), 837. UV-Vis spectra: $\lambda_{max}$/nm ($\varepsilon_{max}$/$mol^{-1}cm^{-1}$). 903 (225), 749 (169), 411 (848), 273 (1136). $\Lambda_M$ ($\Omega^{-1}cm^2\,mol^{-1}$) = 122. $\mu_{eff}$ = 1.76 BM.

**[Cu(NCS)(dbdmp)]]$BF_4$ (6).** Yield. 0.198 g (73 %). Found C = 42.15, H = 5.99, N = 18.22 %. Anal calc for $C_{19}H_{32}N_7SBF_4Cu$: C = 42.19, H = 5.96, N = 18.13%. IR (KBr pellet) $cm^{-1}$; ν($NCS^-$), 2097 vs; ν(C = C) + ν (C = N)/pz ring, 1551 s, 1466 s; ν($BF_4^-$), 1046 br. UV-Vis spectra: $\lambda_{max}$/nm ($\varepsilon_{max}$/$mol^{-1}cm^{-1}$). 900 (220), 736 (206), 379 (1100) 261 (1240). $\Lambda_M$ ($\Omega^{-1}cm^2\,mol^{-1}$) = 125. $\mu_{eff}$ = 1.76 BM.

### 3.2.2.4. [Cu(NCO)(dbdmp)]X, X = $ClO_4^-$ (7), $PF_6^-$ (8), $BF_4^-$(9)

The complexes were prepared by following the same procedure as for complex **1-3** except NaNCO was used instead of $NaN_3$. Blue colored crystals were obtained after slow evaporation of solvent.

**[Cu(NCO)(dbdmp)]$ClO_4$ (7).** Yield. 0.236 g (88 %). Found C = 42.58, H = 5.95, N = 18.43 %. Anal calc for $C_{19}H_{32}N_7O_4ClCu$: C = 42.46, H = 6.0, N = 18.24 %. IR (KBr pellet) $cm^{-1}$; ν($NCO^-$), 2236 vs; ν(C = C) + ν (C = N)/pz ring, 1548 s, 1465 s; $\nu_{asmy}$(Cl–O), 1109 br; δ(O–Cl–O), 623 s. UV-Vis spectra: $\lambda_{max}$/nm ($\varepsilon_{max}$/$mol^{-1}cm^{-1}$). 920 (247), 734 (156), 316 (718), 288 (680). $\Lambda_M$ ($\Omega^{-1}cm^2\,mol^{-1}$) = 120. $\mu_{eff}$ = 1.76 BM.

**[Cu(NCO)(dbdmp)]$PF_6$** (**8**) Yield. 0.245g (84 %). Found C = 39.27, H = 5.59, N = 16.69 %. Anal calc for $C_{19}H_{32}N_7OPF_6Cu$: C = 39.14, H = 5.53, N = 16.82 %. IR (KBr pellet) $cm^{-1}$; ν($NCO^-$), 2241 vs; ν(C = C) + ν (C = N)/pz ring, 1555 s, 1466 s; ν($PF_6^-$), 847 br. UV-Vis spectra: $\lambda_{max}$/nm ($\varepsilon_{max}$/$mol^{-1}cm^{-1}$). 919 (254), 736 (159), 316 (952), 290 (885). $\Lambda_M$ ($\Omega^{-1}cm^2\,mol^{-1}$) = 120. $\mu_{eff}$ = 1.76 BM.

**[Cu(NCO)(dbdmp)]$BF_4$** (**9**). Yield. 0.200 g (76 %). Found C = 43.35, H = 6.22, N = 18.61 %. Anal calc for $C_{19}H_{32}N_7OBF_4Cu$: C = 43.48, H = 6.15, N = 18.68 %. IR (KBr pellet) $cm^{-1}$; ν($NCO^-$), 2234 vs; ν(C = C) + ν (C = N)/pz ring, 1552 s, 1467 s; ν($BF_4^-$), 1066 br. UV-Vis spectra: $\lambda_{max}$/nm ($\varepsilon_{max}$/$mol^{-1}cm^{-1}$). 926 (238), 741 (142), 316 (986), 289 (880). $\Lambda_M$ ($\Omega^{-1}cm^2\,mol^{-1}$) = 123. $\mu_{eff}$ = 1.76 BM.

### 3.2.3. Physical Measurements

The IR spectrums were recorded on a Perkin-Elmer FT-IR spectrometer RX1 spectrum using KBr pellets. The micro analysis (C, H and N) were carried out using a Perkin-Elmer IA 2400 series elemental analyzer. UV-Vis spectra (1200 - 190 nm) were recorded on a Shimadzu 3600 in $CH_3CN$ solution. Solution conductivity were measured in $CH_3CN$ solution ($10^{-3}$ M) using Equip-Tronics conductivity meter (model

no. EQ-660A). Room temperature magnetic susceptibilities of powder samples were measured using a Faraday magnetic balance equipped with a Mettler UMX 5 balance, OMEGA temperature controller with a field strength of 0.8 Tesla using $Hg[Co(SCN)_4]$ as the reference. Cyclic voltammetry studies were carried out using PARSTAT 2273 advanced electrochemical equipment. The cell consisted of three electrodes: platinum working electrode, Pt-wire as counter electrode and Ag/AgCl as reference electrode. Tetraethylammonium tetrafluoroborate (0.1 M) was used as supporting electrolyte.

### 3.2.4. DNA Binding Experiments

All the spectral titration experiments involving interaction of the complexes with CT-DNA were performed in double distilled buffer containing 50 mM Tris – HCl, 150 mM NaCl and adjusted to pH 7.2 with 1M hydrochloric acid. A solution of CT-DNA in buffer gave a ratio of UV absorption at 260 and 280 nm of ca. 1.9 : 1, indicating that DNA was sufficiently free from protein [28]. The DNA concentration per nucleotide was determined by absorption spectroscopy with the molar absorption coefficient 6600 $M^{-1}$ $cm^{-1}$ at 260 nm [29-30].

#### 3.2.4.1. Absorption Spectroscopic Studies

The binding ability of few complexes with CT-DNA is studied by electronic absorption spectroscopy. Absorption titration experiments were performed at constant concentration of the complexes [2.0 x $10^{-4}$ M] with varying the CT-DNA concentration. A control was added with equal quantity of CT-DNA to nullify the absorbance due to the CT-DNA at the measured wavelength. From the absorption titration data, the intrinsic binding constant ($K_b$) of the complexes **1-6** with CT-DNA were determine using Wolfe-Shimer equation [31].

$$[DNA]/(\varepsilon_a - \varepsilon_f) = [DNA]/(\varepsilon_b - \varepsilon_f) + 1/ K_b (\varepsilon_b - \varepsilon_f)$$

Where $\varepsilon_a$, $\varepsilon_f$ and $\varepsilon_b$ correspond to $A_{obsd}$/[Complex], the extinction coefficient for the free complex, and the extinction coefficient for the complex in fully bound form respectively. Plot of $[DNA]/(\varepsilon_a - \varepsilon_f)$ versus [DNA], where [DNA] is the concentration of CT-DNA in base pairs, gives the value of $K_b$ as the ratio of slop to the intercept.

### 3.2.4.2. Fluorescence Spectroscopic Studies

Fluorescence quenching experiments were performed on a model HITACHI, F-7000 fluorescence spectrophotometer at room temperature by adding complex solution at different concentrations to the pretreated DNA-ethidium bromide complex in tris buffer. All the samples were excited at 510 nm and emission was observed between 550-700 nm. The quenching constant was obtained using Stern – Volmer equation [32].

$$I_o/I = 1 + K_{sv}[Q]$$

Where $I_o$ and I are the emission intensities in the absence and presence of the complexes, respectively. $K_{sv}$ is the linear Stern–Volmer quenching constant and [Q] is the total concentration of complexes.

### 3.2.5. Microbial Assay

The antimicrobial screening of Cu(II) complexes were carried out to understand their effect on both the *Gram positive* (*Bacillus subtilis*) and *Gram negative* (*Escherichia coli*) bacteria. Stock solution of Cu(II) complexes of 100 µM, 1 mM, 10 mM concentrations were prepared in DMSO. Bacteria were grown in Luria broth medium and incubated at 37°C for 24 h followed by frequent subculturing to fresh medium and were used for inoculation. Melted Luria Agar along with above three concentrations of Cu(II) complexes were mixed thoroughly and poured in petriplates. After solidification, overnight grown 1% bacterial cultures (*Gram positive* and *Gram negative*) were plated. Petriplates were incubated at 37°C for 24 h. Inhibition was recorded by the bacterial growth on petriplates.

## 3.3. X-ray Crystallography

The details of data collection and some important features of the refinement for the compounds **1, 4, 5** and **7** are given in Table 3.1 and selected bond lengths and angles are given in Table 3.2. Green crystals of suitable size of complexes **1**, **4** and **5** and blue crystals of **7** were obtained by slow evaporation of methanol solution. Data were collected with Mo-$K_\alpha$ radiation ($\lambda$ = 0.71073Å) at 110 K for all complexes on a

Bruker SMART APEX diffractometer equipped with CCD area detector. The data interpretation were processed with SAINT software [33] and empirical absorption correction was applied with SADABS [34] software programs. All structures were solved by direct methods using SHELXTL [35] and refined by the full-matrix least-square based on $F^2$ technique using SHELXL-97[36] program package. All non-hydrogen atoms were refined anisotropically. The positions of the hydrogen atoms were calculated from the difference Fourier map.

**Table 3.1.** Crystallographic data for Complexes **1**, **4**, **5** and **7**.

| | **[Cu($N_3$)(dbdmp)]$ClO_4$ (1)** | **[Cu(NCS)(dbdmp)]$ClO_4$ (4)** | **[Cu(NCS)(dbdmp)]$PF_6$ (5)** | **[Cu(NCO)(dbdmp)]$ClO_4$ (7)** |
|---|---|---|---|---|
| Empirical formula | $C_{18}H_{32}ClCuN_9O_4$ | $C_{19}H_{32}ClCuN_7O_4S$ | $C_{57}H_{96}Cu_3F_{18}N_{21}S_3P_3$ | $C_{19}H_{32}ClCuN_7O_5$ |
| Formula weight | 537.52 | 553.57 | 1797.26 | 537.51 |
| Temperature (K) | 110(2) | 110(2) | 110(2) | 110(2) |
| Wavelength (Å) | 0.71073 | 0.71073 | 0.71073 | 0.71073 |
| Crystal system | Monoclinic | Monoclinic | Monoclinic | Monoclinic |
| Space group | $P2_1/n$ | $P2_1/c$ | $P2_1/c$ | $P2_1/c$ |
| *a* (Å) | 8.4920(6) | 14.9229(17) | 28.580(3) | 8.7057(9) |
| *b* (Å) | 19.3406(14) | 11.9020(14) | 13.5601(13) | 19.0808(19) |
| *c* (Å) | 14.3568(10) | 14.3303(17) | 22.393(2) | 14.2780(14) |
| ~(°) | 90.00 | 90.00 | 90.00 | 90.00 |
| (°) | 91.5070(10) | 97.767(2) | 112.135(2) | 93.386(2) |
| ¥(°) | 90.00 | 90.00 | 90.00 | 90.00 |
| Volume ($Å^3$) | 2357.2(3) | 2521.9(5) | 8038.7(13) | 2367(4) |
| Z | 4 | 4 | 4 | 4 |
| Density ($g/cm^3$) | 1.515 | 1.458 | 1.485 | 1.508 |
| Absorption coefficient ($mm^{-1}$) | 1.085 | 1.094 | 1.016 | 1.081 |
| F(000) | 1124 | 1156 | 3708 | 1124 |
| θ range for data collection (°) | 1.77 to 28.37 | 1.38 to 28.34 | 1.54 to 26.00 | 1.78 to 28.26 |
| Index ranges | $-8 \le h \le 11$, | $-19 \le h \le 19$, | $-35 \le h \le 35$, | $-11 \le h \le 10$, |

| | | | | |
|---|---|---|---|---|
| | -25 ≤ *k* ≤ 20, | -12≤ *k* ≤ 15, | -15 ≤ *k* ≤ 16, | -25 ≤ *k* ≤ 17, |
| | -18 ≤ *l* ≤ 16 | -19 ≤ *l* ≤ 12 | -27 ≤ *l* ≤ 26 | -19 ≤ *l* ≤ 18 |
| Reflections collected | 13898 | 8495 | 42571 | 13933 |
| Independent reflections | 5398 | 3881 | 15734 | 5484 |
| | [R(int) = 0.0188] | [R(int) =0.0342] | [R(int) = 0.0524] | [R(int) = 0.0227] |
| Max. and min. transmission | 0.8287 and 0.7093 | 0.9473 and 0.6688 | 0.9605 and 0.6988 | 0.7970 and 0.6478 |
| Data / restraints / parameters | 5398 / 0 / 304 | 3881 / 0 / 304 | 15734 / 0 / 964 | 5484 / 0 / 304 |
| Goodness-of-fit on $F^2$ | 1.042 | 0.953 | 1.196 | 1.026 |
| Final R indices [I>2sigma(I)] | *R1* = 0.0298, | *R1* = 0.0397, | *R1* = 0.0762, | *R1* = 0.0308, |
| | w*R2* = 0.0773 | w*R2* = 0.0923 | w*R2* = 0.1760 | w*R2* = 0.0819 |
| *R* indices (all data) | *R1* = 0.0330, | *R1* = 0.0478, | *R1* = 0.0981, | *R1* = 0.0335, |
| | w*R2* = 0.0788 | w*R2* = 0.0949 | wR2 = 0.1901 | w*R2* = 0.0836 |
| Largest diff. peak and hole($eA^{-3}$) | 0.397 and -0.309 | 0.479 and -0.293 | 1.810 and -0.598 | 0.398 and -0.265 |
| CCDC | 921665 | 872097 | 872099 | 872098 |

**Table 3.2.** Selected bond lengths (Å) and bond angles (º) for complexes **1**, **4**, **5** and **7**.

| Bond lengths (Å) | | | | | | | |
|---|---|---|---|---|---|---|---|
| **[Cu(N$_3$)(dbdmp)]ClO$_4$ (1)** | | **[Cu(NCS)(dbdmp)]ClO$_4$ (4)** | | **[Cu(NCS)(dbdmp)]PF$_6$ (5)** | | **[Cu(NCO)(dbdmp)]ClO$_4$ (7)** | |
| Cu(1)-N(7) | 1.9450(14) | Cu(1)-N(7) | 1.932(3) | Cu(1)-N(7) | 1.925(4) | Cu(1)-N(7) | 1.9148(15) |
| Cu(1)-N(1) | 2.0685(14) | Cu(1)-N(1) | 2.036(2) | Cu(1)-N(1) | 2.050(4) | Cu(1)-N(1) | 2.0646(14) |
| Cu(1)-N(3) | 2.0696(13) | Cu(1)-N(3) | 2.066(2) | Cu(1)-N(3) | 2.053(4) | Cu(1)-N(3) | 2.0512(13) |
| Cu(1)-N(5) | 2.1121(13) | Cu(1)-N(5) | 2.124(2) | Cu(1)-N(8) | 2.202(4) | Cu(1)-N(5) | 2.1186(14) |
| Cu(1)-N(6) | 2.1125(14) | Cu(1)-N(6) | 2.115(2) | Cu(1)-N(6) | 2.106(4) | Cu(1)-N(6) | 2.1094(13) |

| Bond angles (˚) | | | | | | | |
|---|---|---|---|---|---|---|---|
| **[Cu(N$_3$)(dbdmp)]ClO$_4$ (1)** | | **[Cu(NCS)(dbdmp)]ClO$_4$ (4)** | | **[Cu(NCS)(dbdmp)]PF$_6$ (5)** | | **[Cu(NCO)(dbdmp)]ClO$_4$ (7)** | |
| N(7)-Cu(1)-N(1) | 101.10(6) | N(7)-Cu(1)-N(1) | 100.28(10) | N(7)-Cu(1)-N(1) | 100.48(17) | N(7)-Cu(1)-N(1) | 99.20(6) |
| N(7)-Cu(1)-N(3) | 175.75(6) | N(7)-Cu(1)-N(3) | 177.97(9) | N(7)-Cu(1)-N(3) | 177.63(18) | N(7)-Cu(1)-N(3) | 178.97(6) |
| N(7)-Cu(1)-N(5) | 104.16(6) | N(7)-Cu(1)-N(5) | 100.12(11) | N(7)-Cu(1)-N(6) | 94.86(17) | N(7)-Cu(1)-N(5) | 101.21(6) |
| N(1)-Cu(1)-N(5) | 111.90(5) | N(1)-Cu(1)-N(5) | 111.78(9) | N(1)-Cu(1)-N(6) | 129.70(16) | N(1)-Cu(1)-N(5) | 112.58(5) |
| N(7)-Cu(1)-N(6) | 91.52(6) | N(7)-Cu(1)-N(6) | 93.48(9) | N(7)-Cu(1)-N(4) | 97.54(18) | N(7)-Cu(1)-N(6) | 95.18(6) |
| N(1)-Cu(1)-N(6) | 132.79(5) | N(1)-Cu(1)-N(6) | 130.84(9) | N(1)-Cu(1)-N(4) | 118.69(16) | N(1)-Cu(1)-N(6) | 132.79(5) |
| N(5)-Cu(1)-N(6) | 108.53(5) | N(5)-Cu(1)-N(6) | 111.77(8) | N(6)-Cu(1)-N(4) | 106.10(15) | N(5)-Cu(1)-N(6) | 108.20(5) |

## 3.4. Results and Discussions

### 3.4.1. Syntheses

The mononuclear pseudohalides containing copper(II) complexes [Cu(dbdmp)(X)]Y, (X = $N_3^-$, $NCS^-$, $NCO^-$ and Y = $ClO_4^-$, $PF_6^-$, $BF_4^-$) are readily synthesized through mixing of copper(II) salt like $Cu(ClO_4).6H_2O$ or $Cu(CH_3COO)_2.H_2O$, ligand dbdmp, X ($N_3^-$ / $NCS^-$ / $NCO^-$) and Y ($ClO_4^-$ / $PF_6^-$ / $BF_4^-$) ions in 1 :1 :1: 1 mole ratio in the presence of aqueous methanol at room temperature (Scheme3.1). Molar conductivity measurement in $CH_3CN$ solution (~$10^{-3}$ M) shows all the complexes are 1:1 electrolyte ($\Lambda_M$ ~120 $\Omega^{-1}cm^2\ mol^{-1}$) indicating the presence of counter anion in the molecule and there was no change of molar conductivity even after 2 h indicating no dissociation of the complexes in the solution. The presence of counter anion was proved by IR spectra and single crystal X-ray diffraction studies. All complexes gave satisfactory microanalysis results confirming their composition. The diffraction quality crystals for structural studies were obtained by slow evaporation of the solution. The complexes are moderately soluble in acetonitrile, methanol, ethanol, dichloromethane, acetone etc.

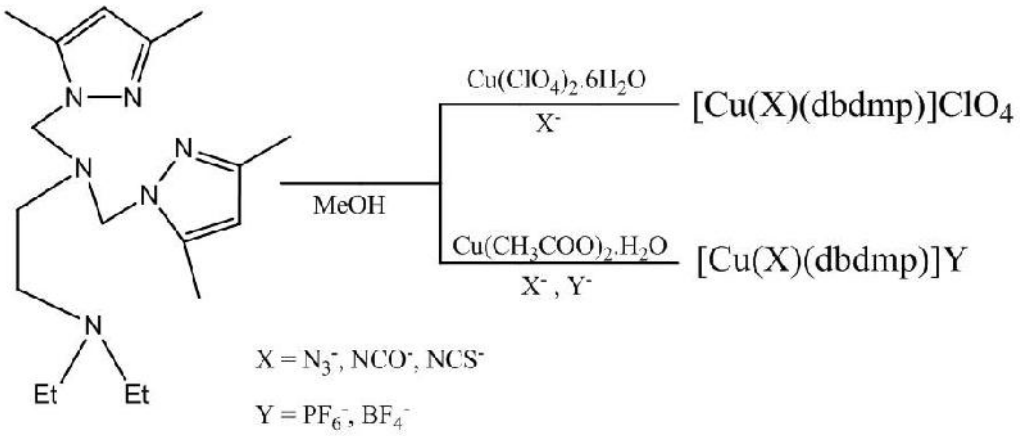


**Scheme.3.1.** Syntheses of complexes.

### 3.4.2. Descriptions of Crystal Structures

The molecular structures of complexes **1, 4, 5** and **7** were determined by the single crystal X-ray diffraction technique. ORTEP diagrams with atom numbering schemes are shown in Fig.3.1. The complexes are crystallized in a monoclinic crystal system with *$P2_1/n$ or $P2_1/c$* space group. In all the complexes ligand dbdmp acts as tetradentate $N_4$-coordinated- being bonded through two tertiary amines nitrogen atoms of *N,N*-diethylethylenediamine and two nitrogen atoms from two pyrazole ring. The central Cu(II) ion is coordinated by five nitrogen donor atoms - four nitrogen from ligand dbdmp and one nitrogen from pseudohalide ions ($N_3^-$ / $NCS^-$ / $NCO^-$) in the complexes. The coordination geometry around the copper is best described as distorted trigonal bipyramidal which is revealed by the magnitude of the trigonality index ($\tau$ = 0.716 – 0.798) for the complexes. For the perfect square pyramidal and trigonal bipyramidal geometries, the $\tau$ - values are zero and unity, respectively [37]. In all the complexes, the basal positions are occupied by one tertiary nitrogen atom N(6) of ligand dbdmp and two pyrazole nitrogen atoms N(1) and N(5) and the axial positions are occupied by another tertiary nitrogen atom N(3) of ligand dbdmp and nitrogen atom N(7) of coordinated pseudohalide ion ($N_3^-$ / $NCS^-$ / $NCO^-$). The terminal pseudohalides ($N_3^-$ / $NCS^-$ / $NCO^-$) are nearly linear to the copper(II) atom with bond angles 175.48(17)º in N(9)-N(8)-N(7) (for $N_3^-$), 179.4(3)º in N(7)-C(19)-S(1) (for $NCS^-$) and 178.0(2)º in N(7)-C(19)-O(1) (for $NCO^-$). The Cu-N bond distances in the basal plane are in the range of 2.036(2) - 2.202(4) Å and the two axial Cu-N distances are in the range of 1.914(15) - 2.069(13) Å in all the complexes. The axial bond angles are in the range of 175.75 to 178.97° and are very close to 180° in the complexes.

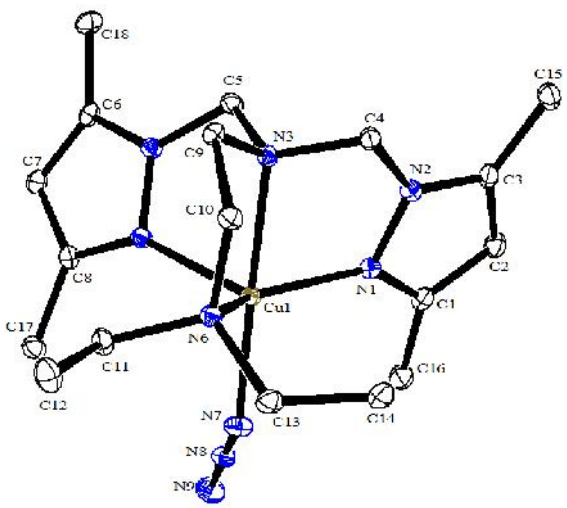


(a) $[Cu(N_3)(dbdmp)]ClO_4$

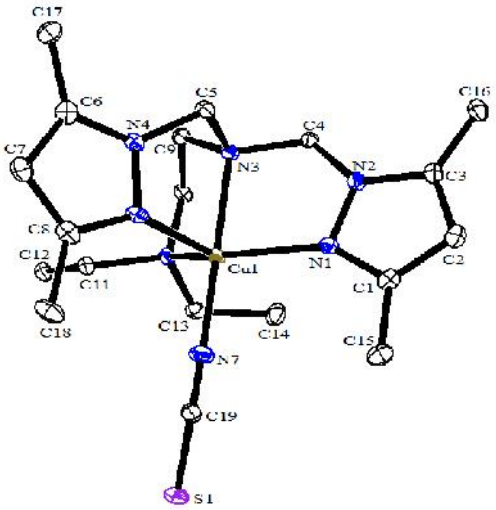


(b) $[Cu(NCS)(dbdmp)]ClO_4$

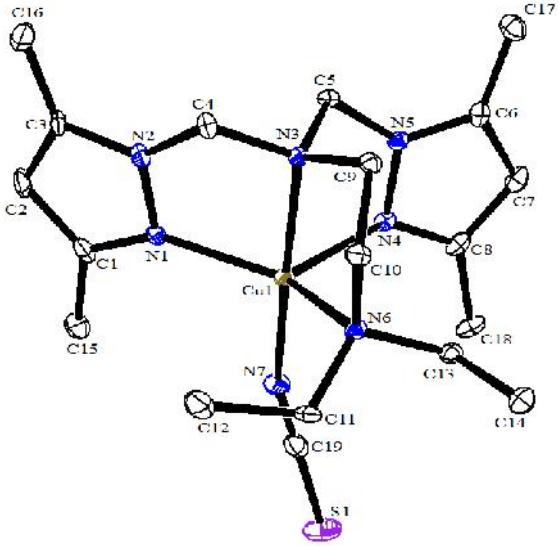


(c) $[Cu(NCS)(dbdmp)]PF_6$

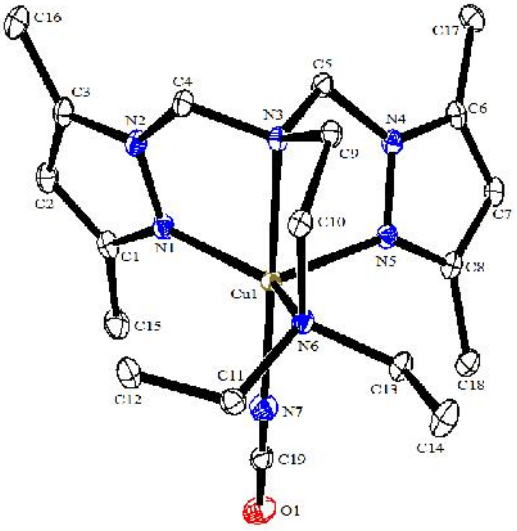


(d) $[Cu(NCO)(dbdmp)]PF_6$

**Fig.3.1.** ORTEP diagram depicting the cationic part of the complexes **1**(a), **4** (b), **5** (c) and **7** (d) with atom numbering scheme (30% probability factor for the thermal ellipsoids, H atoms are omitted for clarity).

### 3.4.3. Spectral Data

#### 3.4.3.1. IR Spectra

The IR spectra of the complexes were assigned in comparison of the spectra of the ligand. All the complexes show two intense bands at ~ 1550 and ~ 1460 $cm^{-1}$ and these two bands are also present in the ligand indicating the coordination of ligand dbdmp in the metal complexes. The complexes **1**-**3** exhibit a very strong band in the region ~ 2053 $cm^{-1}$ which is assigned to asymmetric stretching vibration of N- bonded terminal $\nu(N_3^-)$ band. A strong band in the region of 2234 – 2241 $cm^{-1}$ appeared for complexes **7** - **9** which are assigned to $\nu(NCO^-)$ and at 2092 – 2097 $cm^{-1}$ range appeared for complexes **4** - **6** due to N-bonded ν(NCS). The IR spectra of complexes **1**, **4** and **7** exhibited a broad band at ~ 1100 $cm^{-1}$ due to $\nu_{asym}$(Cl-O) and a weak band at ~ 623 $cm^{-1}$ due to δ(O-Cl-O) confirming the presence of perchlorate ion outside the coordination sphere in the complexes. Similarly, complexes **2**, **5**, and **8** show a strong band at ~ 845 $cm^{-1}$ due to $\nu(PF_6^-)$ and complexes **3**, **6** and **9** exhibited a broad band in the region of ~ 1065 $cm^{-1}$ due to $\nu(BF_4^-)$ indicating the presence of $PF_6^-$ and $BF_4^-$ anion, respectively in the complexes.

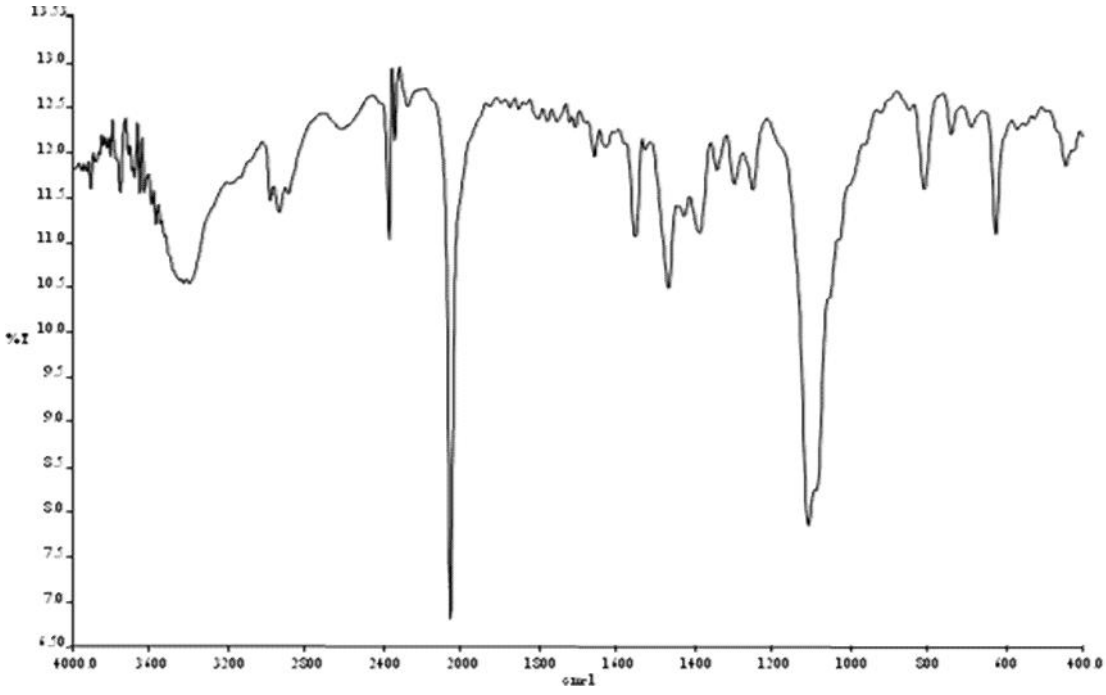


**Fig.3.2.** IR spectrum of $[Cu(N_3)(dbdmp)]ClO_4$ **(1)**.

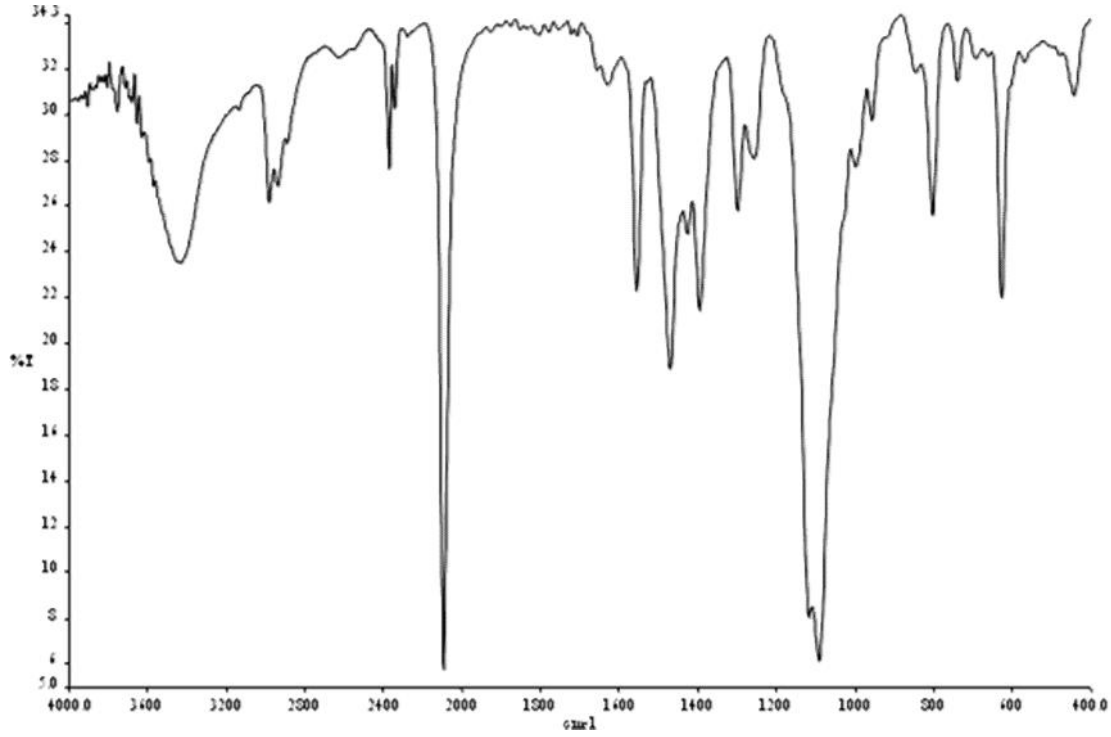


**Fig.3.3.** IR spectrum of $[Cu(NCS)(dbdmp)]ClO_4$ **(4)**.

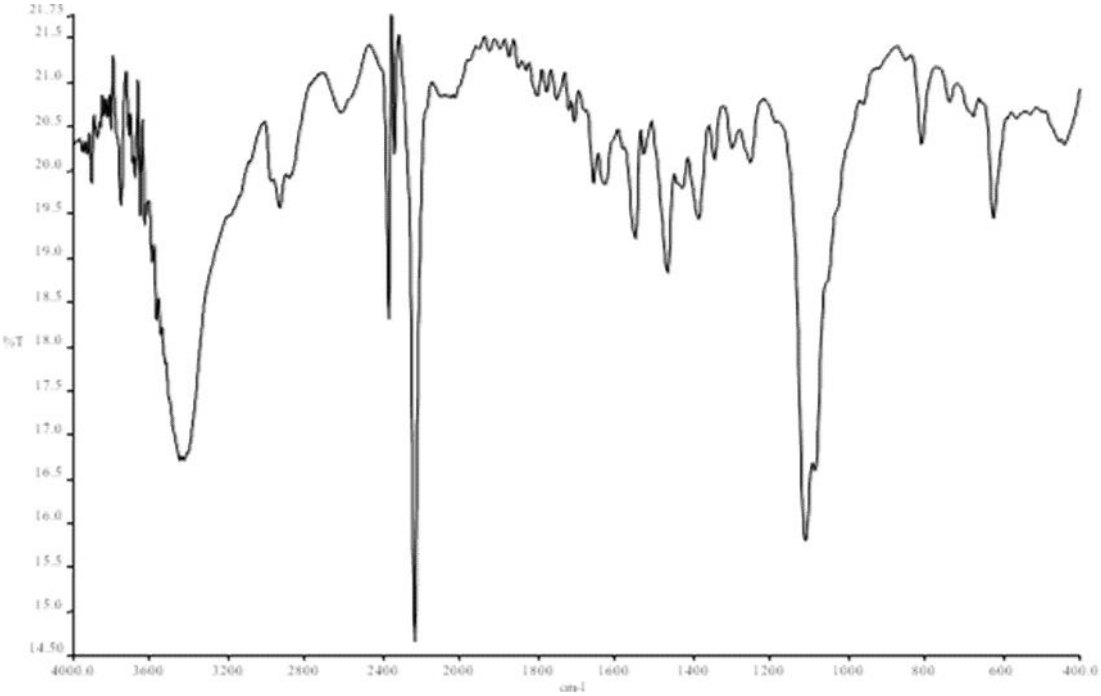


**Fig.3.4.** IR spectrum of $[Cu(NCO)(dbdmp)]ClO_4$ **(7)**.

### 3.4.3.2. Electronic Spectra

The UV-Visible spectra of the complexes (Fig.3.5) **1** - **9** were recorded in $CH_3CN$ ($10^{-3}$ M) and corresponding $\lambda_{max}$ and molar absorption coefficient are given in Table 3. For all complexes, a broad absorption band was observed at λ > 800 nm ($d_{xy,}\ d_{x^2-y^2} \rightarrow d_{z^2}$) and a weak transition ($d_{xy}$, $d_{yz} \rightarrow d_{z^2}$) at higher energy region (λ < 750 nm). For azide complexes **1** - **3**, one broad absorption band in the region of 910 - 915 nm (ε ~ 70 - 75 $mol^{-1}cm^{-1}$) and a shoulder at ~ 707 nm (ε ~107 - 150 $mol^{-1}cm^{-1}$) were observed. Similar absorption band was obtained for thiocyanate containing complexes **4** - **6** at ~ 900 nm (ε ~ 225 $mol^{-1}cm^{-1}$) and at ~ 740 nm (ε ~ 170 $mol^{-1}cm^{-1}$) and isocyanate complexes **7** – **9** at 920 nm (ε ~ 247 $mol^{-1}cm^{-1}$) and at 736 nm (ε ~ 150 $mol^{-1}cm^{-1}$). This type of spectral feature is typical for Cu(II) complexes with trigonal bipyramidal geometry [38-43].

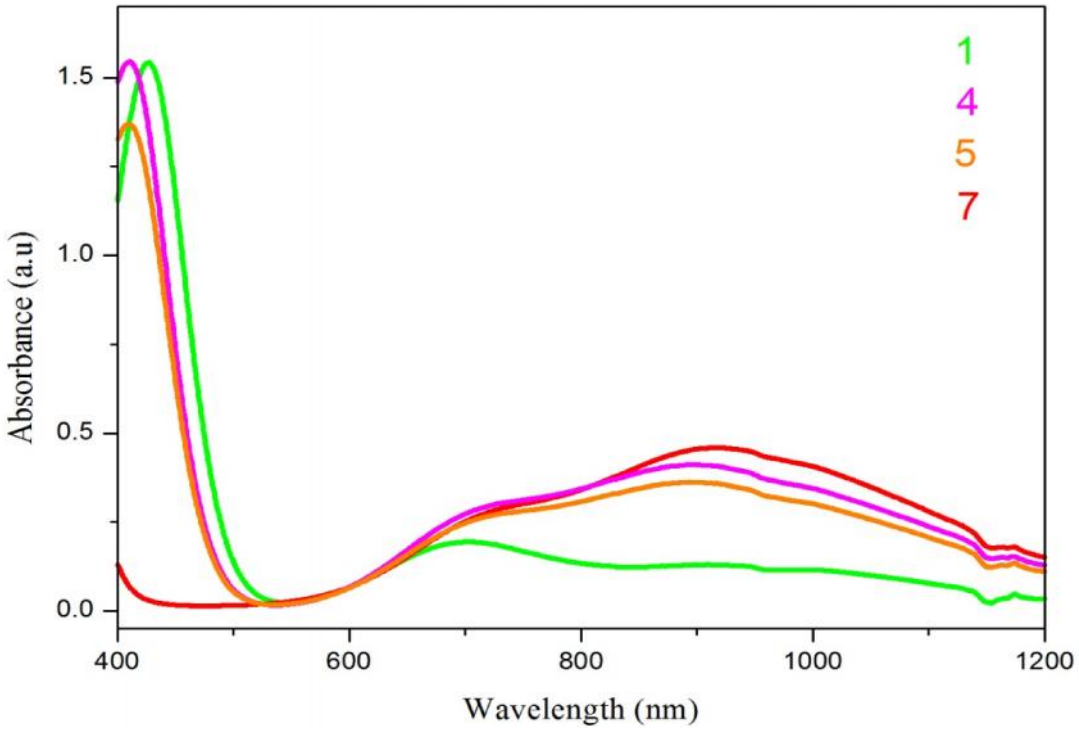


**Fig.3.5.** Electronic spectra of complexes **1**, **4**, **5** and **7** in $CH_3CN$ ($10^{-3}$ M).

Generally, square pyramidal or distorted square pyramidal Cu(II) complexes show spectral band in the region of 550 - 660 nm ($d_{xz}$, $d_{yz} \rightarrow d_{x^2-y^2}$). Absence of spectral band in the region in all the complexes also indicate the geometry around copper(II) center is trigonal bipyramidal. The electronic spectral data (Table 3.3)

indicates that $\lambda_{max}$ of the complexes increases in the order of $NCO^- > N_3^- > NCS^-$. Therefore, the energy of the d-d transitions are in the order of $NCS^- > N_3^- > NCO^-$. This energy change is due to the reduction of ligand field strength of the $NCS^-$ / $N_3^-$ / $NCO^-$ in the complexes. It is also observed that bathochromic shift of 4 to 15 nm when the counter anion of the complexes changes from $ClO_4^-$ to $PF_6^-$ to $BF_4^-$ for a particular pseudohalide ion. There is also no change of $\lambda_{max}$ in solution indicating no dissociation or change of geometry after dissolution.

**Table 3.3.** Electronic Spectral data of complexes **1** - **9** in $CH_3CN$ ($10^{-3}$ M).

| **Complex** | $\lambda_{max}$ **(nm)** ($\varepsilon_{max}$/mol$^{-1}$cm$^{-1}$) |
|---|---|
| $[Cu(N_3)(dbdmp)]ClO_4$ **(1)** | 911 (70), 703 (108), 427 (830), 281(1344) |
| $[Cu(N_3)(dbdmp)]PF_6$ **(2)** | 917 (85), 707 (137), 428 (935), 282 (1306) |
| $[Cu(N_3)$ (dbdmp)$]BF_4$ **(3)** | 920 (90),707 (157), 429 (1108), 282 (1353) |
| $[Cu(NCS)(dbdmp)]ClO_4$ **(4)** | 896 (228), 727 (167), 411 (855), 271 (1154) |
| $[Cu(NCS)$ (dbdmp)$]PF_6$ **(5)** | 903 (225), 749(169), 411 (848), 273 (1136) |
| $[Cu(NCS)$ (dbdmp)$]BF_4$ **(6)** | 900 (220), 736 (206), 379 (1100), 273 (1135) |
| $[Cu(NCO)(dbdmp)]ClO_4$ **(7)** | 920 (247), 734 (156), 316 (718), 288 (680) |
| $[Cu(NCO)(dbdmp)]PF_6$ **(8)** | 919 (254), 736 (159), 316 (952), 290 (885) |
| $[Cu(NCO)(dbdmp)]BF_4$ **(9)** | 926 (238), 741 (142), 316 (986), 289 (880) |

### 3.4.4. Cyclic Voltammetry and Magnetic Data

The electrochemcial behavior of the complexes **1**, **4** and **7** have been examined by cyclic voltammetry using platinum electrode in $CH_3CN$ solution (~ $10^{-3}$ M) using tetraethyl ammonium tetrafluoroborate as supporting electrolyte in the potential range 2.0 to -2.0 V versus Ag/AgCl reference electrode. It show complexes **1** and **4** display a reduction process with $E_{1/2}$ values at -0.449 and -0.338 V corresponding to a Cu(II)/Cu(I) electron transfer. The peak potential separation ($\Delta E_p$) is 0.197 and 0.238 V at a scan rate 100 mV/s, indicating quasi-reversible one-electron transfer process. The complex **7** shows irreversible reduction of Cu(II)/Cu(I) with $E_{pc}$ -0.631 V.

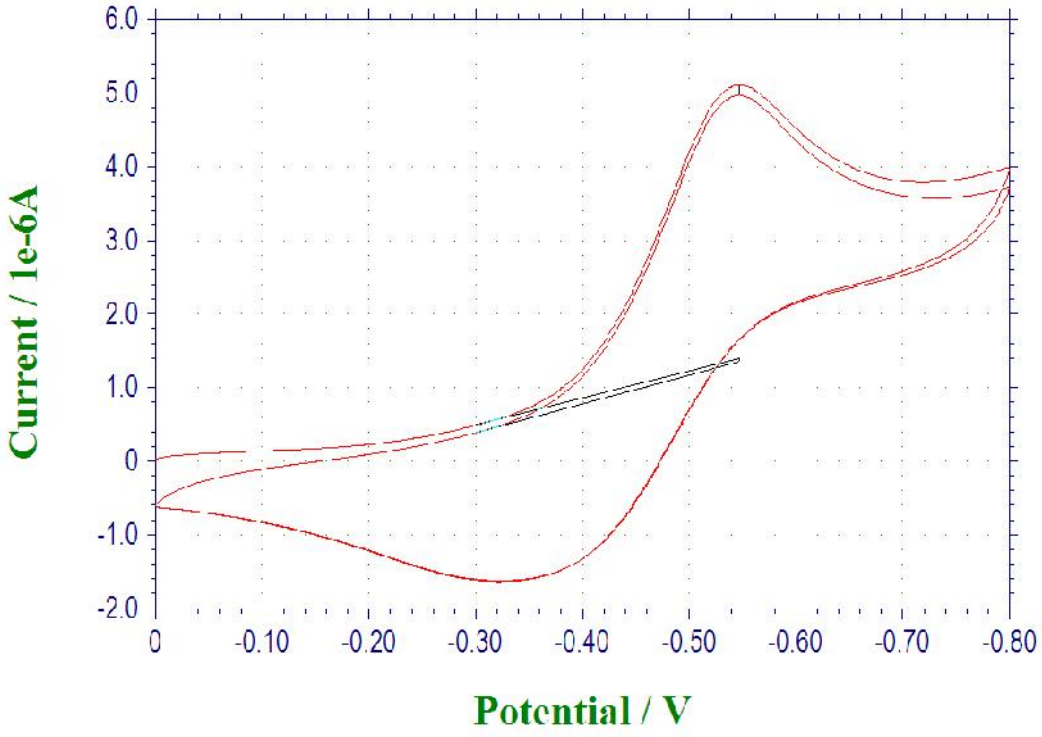


**Fig.3.6.** Cyclic voltammogram of complex **1** at 100 $mVs^{-1}$ using platinum electrode in $CH_3CN$ contained 1 mM complex and 0.1M $Et_4NBF_4$.

The room temperature magnetic moment of the complexes show «$_{eff}$ of all the samples ~ 1.78 BM indicating one electron paramagnetism and this is typical for all copper(II) complexes.

### 3.4.5. DNA binding experiments

#### 3.4.5.1. Electronic absorption titration

The binding ability of complexes **1, 2, 4, 5, 7** and **8** with CT-DNA are studied by measuring their effects using the electronic absorption spectroscopy which is the most useful technique for studying the binding modes of metal complexes with DNA. Complex binding with DNA usually results in hypochromism and blue shift arising from strong stacking interaction between complex and DNA [44-48].

The extent of hypochromism gives a measure of the intercalative binding. In the electronic absorption titration experiments, when the complexes are titrated with CT-DNA, interesting spectral changes are observed in the ligand based bands. In the complex **1** intensity of the spectral band at 424 nm shows hypochromism with blue shift on the addition of CT-DNA as shown in the Fig.3.7. Such spectral changes in intraligand transition are due to surface binding [49]. Similar types of spectral changes were also observed for the complexes **2**, **4, 5, 7** and **8** as shown in the Fig.3.7 and Fig.3.8.

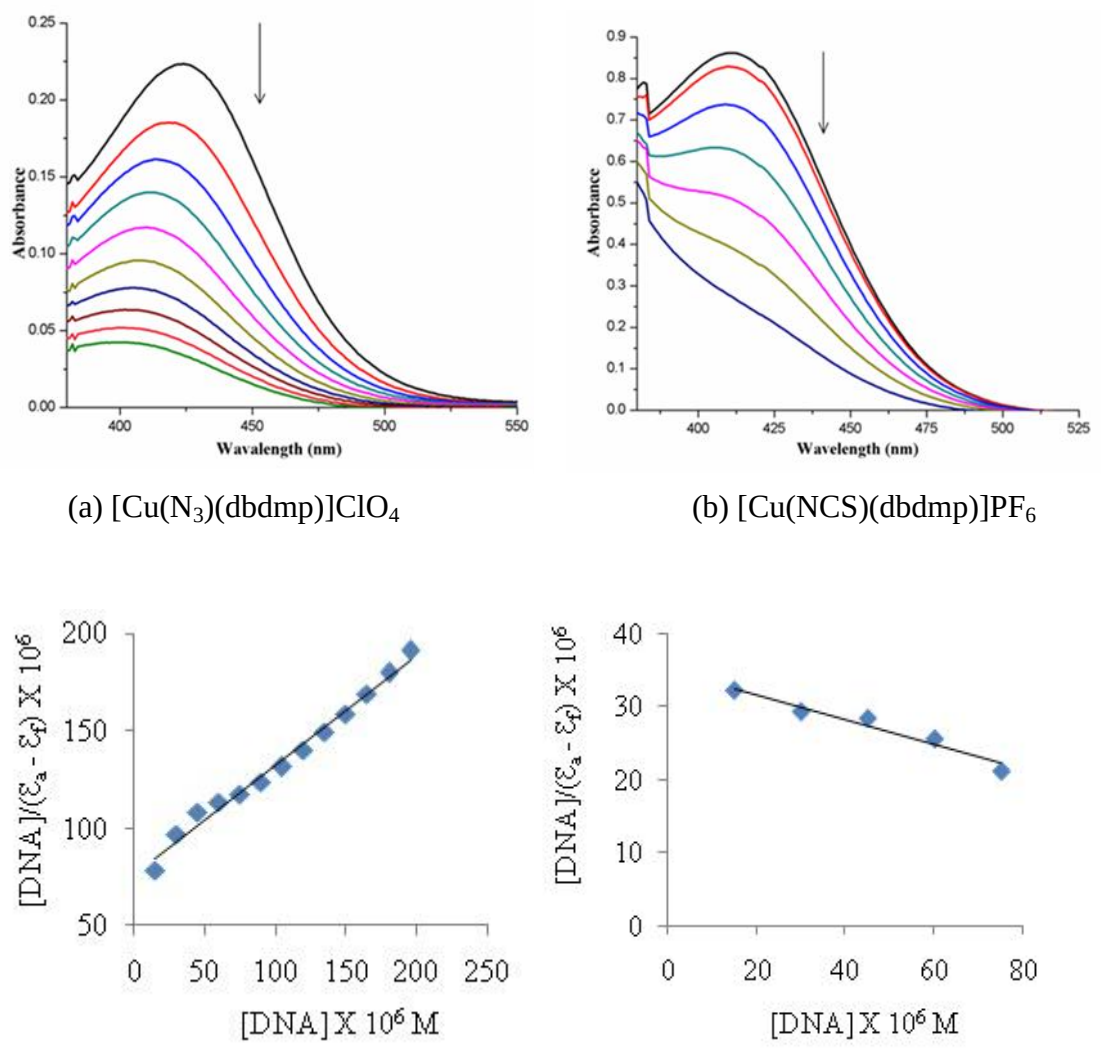


(a) $[Cu(N_3)(dbdmp)]ClO_4$ (b) $[Cu(NCS)(dbdmp)]PF_6$

(c) (d)

**Fig.3.7.** Absorption spectra of complexes **1** (a) and **4** (b) (2 x $10^{-4}$ M) in the absence and presence of increasing amounts of CT-DNA (0-200 μM) at 25°C in Tris-HCl/NaCl buffer (pH 7.2). Arrow shows the absorbance changing upon increasing DNA concentrations. Least-squares fit of [DNA]/(Ɛa - Ɛf) vs. [DNA] for the complexes **1**(c) and **4** (d).

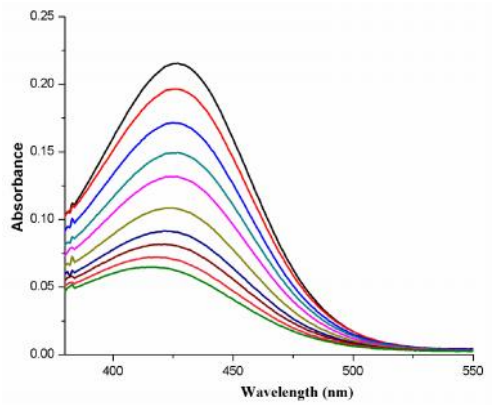


(a) $[CuN_3(dbdmp)]PF_6$

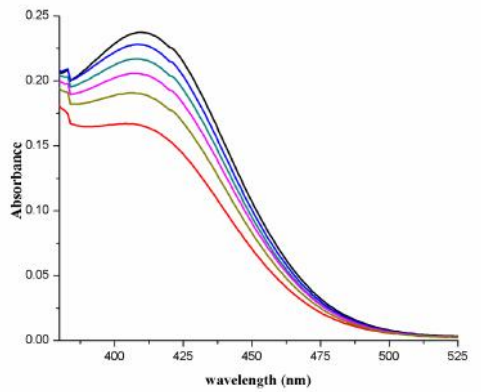


(b) $[Cu(NCS)(dbdmp)]PF_6$

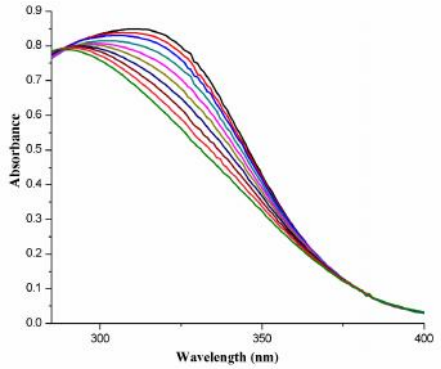


(c) $[Cu(NCO)(dbdmp)]ClO_4$

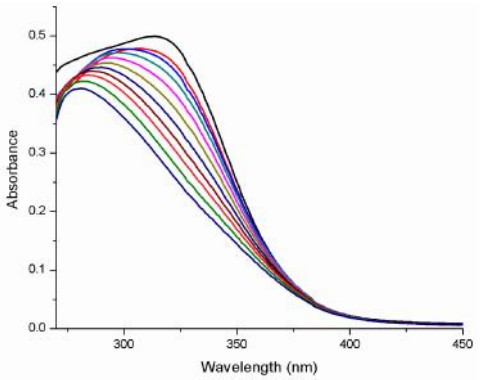


(d) $[Cu(NCO)(dbdmp)]PF_6$

**Fig.3.8.** Absorption spectra of the complexes **2** (a), **5** (b), **7** (c) and **8** (d) in the presence of CT-DNA.

The $K_b$ values (Table 3.4) of complexes also support the strong binding of these complexes to CT-DNA. The exact mode of binding cannot be proposed by UV spectroscopic titration studies. In most cases, the existence of hypochromism for all complexes could be considered as first evidence that the binding of the complexes involving intercalation between the base pairs of CT-DNA cannot be ruled out [50-55].

### 3.4.5.2. Fluorescence spectral studies

As the present complexes are non-fluorescent on excitation in the UV-visible region, competitive ethidium bromide binding experiments were carried out to gain support for the extent of binding with plasmid DNA. Ethidium bromide (EB) is a weak chromophore but it was shown to emit intense fluorescence light when it

strongly intercalated into the base pairs of double-stranded DNA. It is proved that fluorescent light could be quenched by the addition of a second molecule [56]. When a complex is intercalated to EB-bound DNA, it decreases the emission intensity of EB-DNA complex as it releases the EB from DNA and reduced emission intensity is used as a measure of DNA binding ability of the complex. This behavior can be analyzed through Stern-Volmer equation [57]. The emission spectra of EB bound to DNA in the absence and presence of each complex were recorded in the Tris-buffer. The fluorescence quenching curve of EB-bound to DNA by the complexes **1** and **4** are shown in the Fig.3.9 and the reduction in the intensity of the emission band indicates that the complex competes with EB and strongly binds with DNA through intercalation. The Stern–Volmer plots of DNA–EB (Fig.3.9) illustrate that the quenching of EB-DNA fluorescence by the compounds are in good agreement (R = 0.9) with the linear Stern–Volmer equation [50-52, 57] which also suggest the strong binding of the complexes with DNA. The Stern-Volmer quenching constant values (Table 3.4) are less than the binding constant of the classical intercalators and metallointercalators ($10^7$ $M^{-1}$) [58]. Similar types of spectral changes were also observed for the complexes **2**, **5, 7** and **8** as shown in the Fig.3.10.

**Table 3.4.** CT - DNA binding parameters of complexes.

| Complex | $K_b$ ($M^{-1}$) | $K_{sv}$($M^{-1}$) |
|---|---|---|
| $[Cu(N_3)(dbdmp)]ClO_4$ **(1)** | $8.57 \times 10^5$ | $2.3 \times 10^3$ |
| $[Cu(N_3)(dbdmp)]PF_6$ **(2)** | $7.70 \times 10^5$ | $2.6 \times 10^3$ |
| $[Cu(NCS)(dbdmp)]ClO_4$ **(4)** | $4.25 \times 10^5$ | $4.0 \times 10^3$ |
| $[Cu(NCS)(dbdmp)]PF_6$ **(5)** | $3.50 \times 10^5$ | $2.7 \times 10^3$ |
| $[Cu(NCO)(dbdmp)]ClO_4$ **(7)** | $11.50 \times 10^5$ | $3.6 \times 10^3$ |
| $[Cu(NCO)(dbdmp)]PF_6$ **(8)** | $6.80 \times 10^5$ | $2.9 \times 10^3$ |

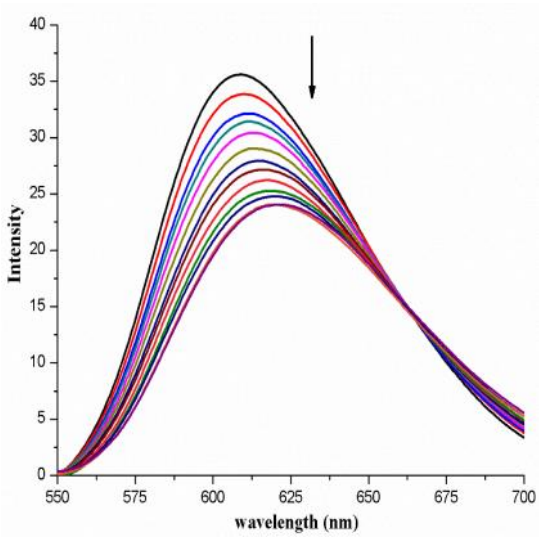


(a) $[Cu(N_3)(dbdmp)]ClO_4$

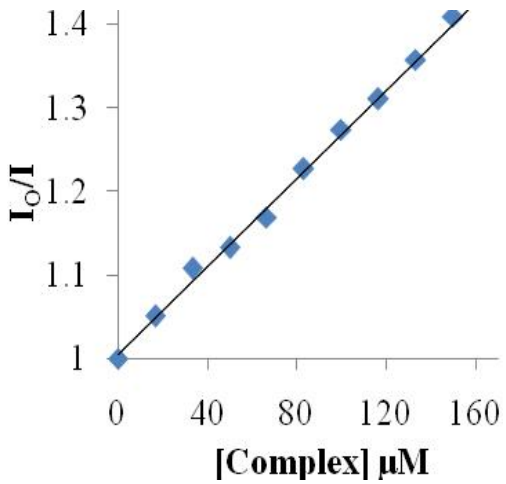


(c)

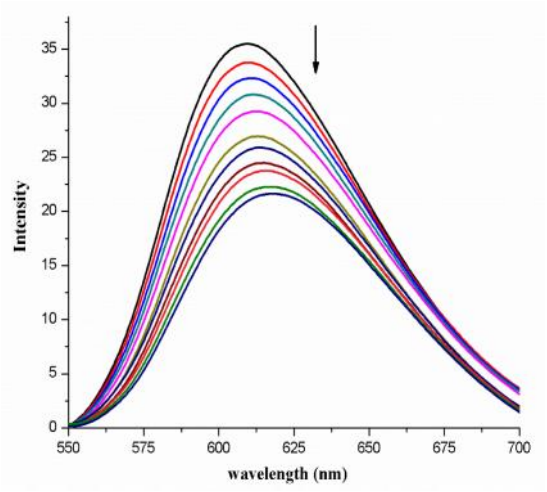


(b) $[Cu(NCS)(dbdmp)]ClO_4$

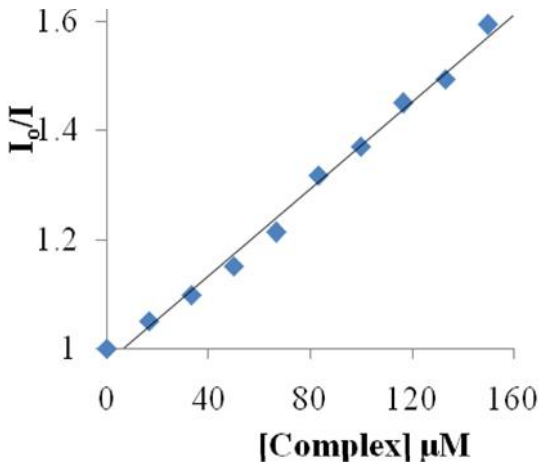


(d)

**Fig.3.9.** Fluorescence quenching spectra of complexes **1** (a) and **4** (b) ($\lambda_{ex}$ = 510 nm) by addition of increasing amount of complexes (0-160 µM) to EB-bound CT-DNA. The plot of $I_o/I$ vs [complex] for complexes **1** (c) and **4** (d).

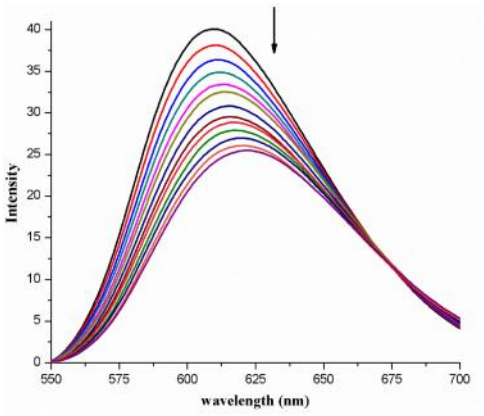


(a) $[Cu(N_3)(dbdmp)]PF_6$

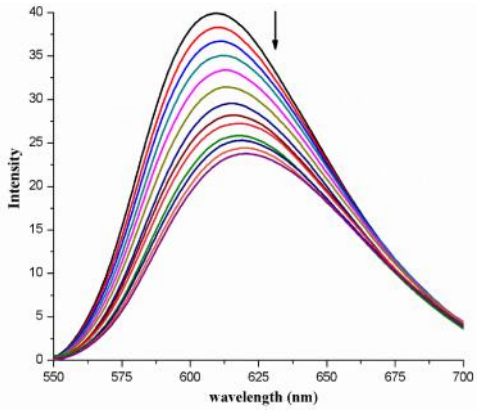


(b) $[Cu(NCS)(dbdmp)]PF_6$

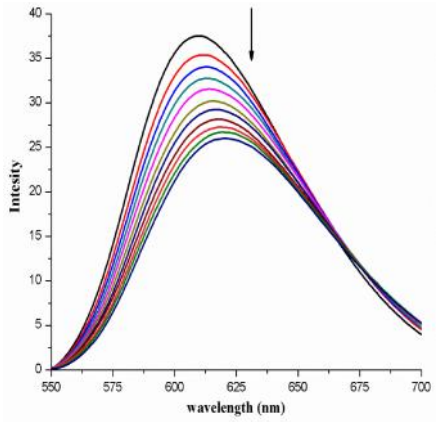


(c) $[Cu(NCO)(dbdmp)]ClO_4$

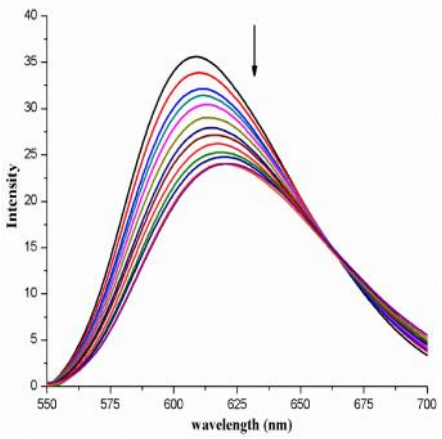


(d) $[Cu(NCO)(dbdmp)]PF_6$

**Fig.3.10.** Fluorescence quenching curves of the EB bound CT-DNA in the presence of complexes **2** (a), **5** (b), **7** (c) and **8** (d).

### 3.4.6. Microbial activity

Dilution methods are routinely used to determine the minimum inhibitory concentrations (MICs) of antimicrobial agents. In dilution tests, microorganisms are tested for their ability to produce visible growth on a series of agar plates or in microwell plates of broth containing dilutions of the antimicrobial agent. The lowest concentration of an antimicrobial agent that will inhibit the visible growth of a

microorganism is known as the MIC. In presence of only DMSO (in which the test solutions were prepared) and $Cu(ClO_4)_2.6H_2O$ both the Gram positive and Gram negative bacteria were able to grow. Complexes **1, 2, 4, 5, 7, 8** and ligand dbdmp with 100 µM concentration were not inhibiting bacterial growth and the bacterial strains were able to grow normally, whereas at 10 mM concentration the same complexes were completely inhibiting bacterial growth of both the strains [Fig.3.11]. Complexes **1** and **4** were inhibiting bacterial growth of even at 1 mM concentration. It means that complexes containing counter anion $ClO_4^-$ and co-ligand $N_3^-$ / $NCS^-$ have best inhibition activity.

From the antimicrobial studies, it can be concluded that all the complexes have higher activity than the organic ligand dbdmp and metallation is essential for inhibition activity. The increased reactivity of the complexes can be explained by Tweedy chelation theory [59]. In a complex, the positive charge of the metal ion is partially share with the donor atom of the ligand and the chelation enhances the lipophilic character of the metal complexes. The lipophilicity increases the penetration power of the complexes into the bacterial cell membrane and blocks the metal binding sites in enzyme of microorganism and also disturbs the respiration process and protein synthesis in the cell and finally restricts further growth of the microorganisms [60-61].

### 3.5. Conclusions

A new series of mononuclear copper(II) complexes of the type $[Cu(X)(dbdmp)]Y$, where X = $N_3^-$ / $NCS^-$ / $NCO^-$, Y = $ClO_4^-$ / $PF_6^-$ / $BF_4^-$ and dbdmp = $N_4$-coordinated ligand *N*,*N*-diethyl-*N'*,*N'*-bis((3,5-dimethyl-*1H*-pyrazol-1-yl)methyl)ethane-1,2-diamine have been synthesized and characterized. Structural studies show all the complexes have distorted trigonal bipyramidal geometry. CT-DNA binding study of the copper(II) complexes were investigated by absorption and fluorescence spectroscopy methods. The results indicate that the complexes can interact strongly with DNA base pair. Antibacterial study of the complexes showed the complete inhibition activity against *Gram positive* (*Bacillus subtilis)* and *Gram negative* (*Escherichia coli*) bacteria at high concentration.

**Fig.3.11.** Photographs of bacterial studies.

| | ***DHSα* strain of *E. coli*** | | | ***B. subtilis*** | | |
|---|---|---|---|---|---|---|
| **Growth of strain** |  | | |  | | |
| ***concentration*** | **100 µM** | **1 mM** | **10 mM** | **100 µM** | **1 mM** | **10 mM** |
| **$Cu(ClO_4).6H_2O$** |  |  |  |  |  |  |
| **Ligand dbdmp** |  |  |  |  |  |  |
| **1** | 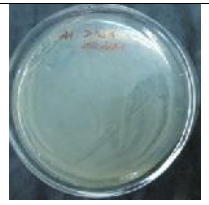 | 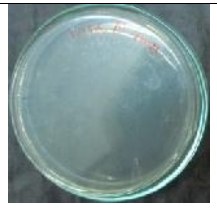 |  |  |  |  |

| | | | | | | |
|---|---|---|---|---|---|---|
| **2** | 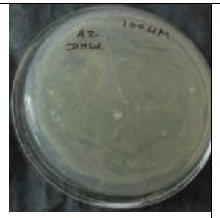 | 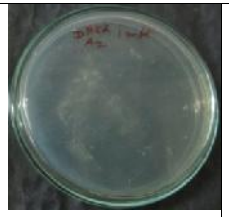 | 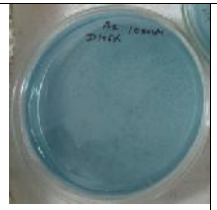 |  |  | 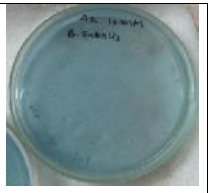 |
| **3** |  |  | 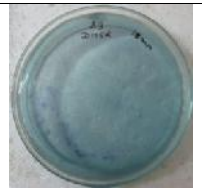 |  |  | 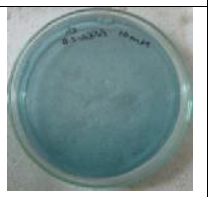 |
| **4** |  |  |  | 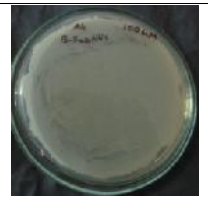 | 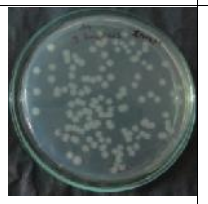 |  |
| **5** |  | 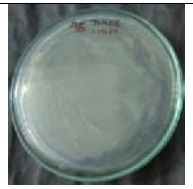 | 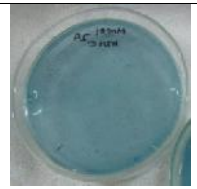 |  |  |  |
| **6** |  |  |  |  | 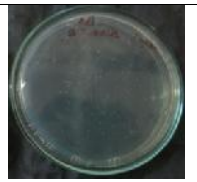 | 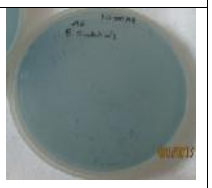 |

## 3.6. References :


1. T. Gupta, S. Dhar, M. Nethaji, A.R. Chakravarty, *Dalton Trans.* (2004) 1896.
2. B. M. Zeglis, V. C. Pierre, J. K. Barton, *Chem. Commun.* (2007) 4565.
3. K. E. Erkkila, D. T. Odom, J. K. Barton, *Chem. Rev.* 99 (1999) 2777.
4. P. J. Dardlier, R. E. Holmlin, J. K. Barton, *Science* 275 (1997) 1465.
5. D. B. Hall, R. E. Holmlin, J. K. Barton, *Nature* 382 (1996) 731.
6. Q.-L. Zhang, J.-G. Liu, H. Chao, G.-Q. Xue, L.-N. Ji, *J. Inorg. Biochem.* 83 (2001) 49.
7. C.-L. Liu, M. Wang, T.-L. Zhang, H.-Z. Sun, *Coord. Chem. Rev.* 248 (2004) 147.
8. K. S. Ksaprzak, *Chem. Res. Toxocol.* 4 (1991) 604.
9. E. L. Hegg, J. N. Burstyn, *Inorg. Chem.* 35 (1996) 7474.
10. A. Panja, *Polyhedron* 43 (2012) 22.
11. S. Anbu, M. Kandaswamy, *Inorg. Chim. Acta* 385 (2012) 45.
12. A. Terenzi, G. Barone, A. Silvestri, A. M. Giuliani, A. Ruggirello, V. T. Liveri, *J. Inorg. Biochem.* 103 (2009) 1.
13. R. S. Kumar, S. Arunachalam, *Eur. J. Med. Chem.* 44 (2009) 1878.
14. V. Uma, A. Castineiras, B. U. Nair, *Polyhedron* 26 (2007) 3008.
15. M. Shakir, M. Azam, Y. Azim, S. Parveen, A. U. Khan, *Polyhedron* 26 (2007) 5513.
16. R. Kumar, S. Arunachalam, *Polyhedron* 25 (2006) 3113.
17. V. Uma, M. Kanthimathi, T. Weyhermuller, B. U. Nair, *J. Inorg. Biochem.* 99 (2005) 2299.
18. Y. G. Fang, J. Zhang, S. Y. Chen, N. Jiang, H. H. Lin, Y. Zhang, X.-Q. Yu, *Bioorg. Med. Chem.* 15 (2007) 696.
19. S. S. Mandal, U. Varshney, S. Bhattacharya, *Bioconjucate Chem.* 8 (1997) 798.
20. M. A. Tsiaggali, E. G. Andreadou, A. G. Hatzidimitriou, A. A. Pantazaki, P. Aslanidis, *J. Inorg. Biochem.* 121 (2013) 121.
21. J. He, J. Sun, Z. W. Maoa, L. N. Ji, H. Sun, *J. Inorg. Biochem.* 103 (2009) 851.
22. M. Zampakou, M. Akrivou, E. G. Andreadou, C. P. Raptopoulou, V. Psycharis, A. A. Pantazaki, G. Psomas, *J. Inorg. Biochem.* 121 (2013) 88.
23. P. M. May, D. R. Williams, in: H. Sigel (Ed.), *Metal Ions in Biological Systems, vol. 12, Marcel Dekker, New York* (1981).
24. H. Sigel (Ed.), *Metal Ions in Biological Systems, vol. 13, Marcel Dekker, New York* (1981).
25. T. Miura, A. Hori-i, H. Mototani, H. Takeuchi, *Biochemistry* 38 (1999) 11560.
26. P. Jaividhya, R. Dhivya, M. A. Akbarsha, M. Palanlandavar, *J. Inorg. Biochem.* 114 (2012) 94.

27. G.-Y. Li, K.-J. Du, J.-Q. Wang, J.-W. Liang, J._F. Kou, X.-J. Hou, L.-N. Ji, H. Chao, *J. Inorg. Biochem.* 119 (2013) 43.
28. J. Marmur, *J. Mol. Biol.* 211 (1961) 3208.
29. M. F. Reichmann, S. A. Rice, C. A. Thomas, P. Doty, *J. Am. Chem. Soc.* 76 (1954) 3047.
30. O. Gia, S. M. Magno, H. Gonzalaz-Diaz, E. Quezada, L. Santana, E. Uriarte,L. Dalla Via, *Bioorg. Med. Chem.* 13 (2005) 809.
31. A. M. Pyle, J. P. Rehmann, R. Meshoyrer, C. V. Kumar, N. J. Turro, J. K. Barton, *J. Am. Chem. Soc.* 111 (1989) 3051.
32. J. R. Lakowicz, G. Webber, *Biochemistry* 12 (1973) 4161.
33. G. M. Sheldrick. SAINT, 5.1 ed. *Siemens Industrial Automation Inc., Madison, WI* (1995).
34. G. M. Sheldrick. SADABS, *Empirical Absorption Correction Program, University of Gottingen, Gottingen, Germany* (1997).
35. G. M. Sheldrick. SHELXTL Reference Manual (Version 5.1), *Bruker AXS, Madison, WI* (1997).
36. G. M. Sheldrick. SHELXL-97: *Program for Crystal Structure Refinement, University of Gottingen, Gottingen* (1997).
37. A. W. Addision, T. N. Rao, J. Reedijk, J. Van Rijn, G. C. Verschoor, *J. Chem. Soc., Dalton Trans.* (1984) 1349.
38. U. Mukhopadhayay, I. Bernal, S. S. Massoud, F. A. Moutner, *Inorg. Chim. Acta* 357 (2004) 3673.
39. S. S. Massoud, F. A. Moutner, M. A. M. Abu-Youssef, N. M. Shuaib, *Polyhedron* 18 (1999) 2061.
40. B. J. Hathaway. in: G. Wilkinson, R. D. Gillard, J. A. McCleverty (Eds.)., *In Comprehensive Coordination Chemistry, Pergamon Press, Oxford, England* 5 (1987) 533.
41. A. M. Dittler-Klingermann, C. Orvig, F. E. Hahn, F. Thanler, C. D. Hubbard, R. van Eldik, S. Schindler, I. Fabian, *Inorg. Chem.* 35 (1996) 7798.
42. F. Thaler, C. D. Hubbard, F. W. Heinemann, R. van Eldik, I. Fabian, Dittler-Klingermann, *Inorg. Chem.* 37 (1998) 4022.
43. F. A. Moutner, C. N. Landry, A. A. Gallo, S. S. Massoud, *J. Mol. Struct.* 837 (2007) 72.
44. C. Hiort, P. Lincoln, B. Norden, *J. Am. Chem. Soc.* 115 (1993) 3448.
45. L. Fin, P. Yang, *J. Inorg. Biochem.* 68 (1997) 79.
46. Mudasir, K. Wijaya, D. H. Tjahjono, N. Yoshioka, H. Inoue, *Z. Naturforsch. 59b* (2004) 310.

47. M. Navarro, E. J. Cisneros-Fajardo, M. Fernandez-Mestre, D. Arrieche, E. Marchan, *J. Biol. Inorg. Chem.* 8 (2003) 401.
48. R. B. Nair, E. S. Teng, S. L. Kirkland, C. J. Murphy, *Inorg. Chem.* 37 (1998) 139.
49. P. T. Selvi, H. S.- Evans, M. Palaniandavar, *J. Inorg. Biochem.* 99 (2005) 2110.
50. K. C. Skyrianou, F. Perdih, I. Turel, D. P. Kessissoglou, G. Psomas, *J. Inorg. Biochem.* 104 (2010) 161.
51. K. C. Skyrianou, V. Psycharis, C. P. Raptopoulou, D. P. Kessissoglou, G. Psomas, *J. Inorg. Biochem.* 105 (2011) 63.
52. A. Tarushi, C. P. Raptopoulou, V. Psycharis, A. Terzis, G. Psomas, D. P. Kessissoglou, *Bioorg. Med. Chem.* 18 (2010) 2678.
53. G. Psomas, A. Tarushi, E. K. Efthimiadou, Y. Sanakis, C. P. Raptopoulou, N. Katsaros, *J. Inorg. Biochem.* 100 (2006) 1764.
54. A. Tarushi, G. Psomas, C. P. Raptopoulou, D. P. Kessissoglou, *J. Inorg. Biochem.* 103 (2009) 898.
55. B. C. Baguley, M. Lebret, *Biochemistry* 23 (1984) 937.
56. J. R. Lakowicz, G. Webber, *Biochemistry* 12 (1973) 4161.
57. G. Psomas, *J. Inorg. Biochem.* 102 (2008) 1798.
58. M. Cory, D. D. McKee, J. Kagan, D. W. Henry, J. A. Miller, *J. Am. Chem. Soc.* 107 (1985) 2528.
59. B. G. Tweedy, *Phytopathology* 55 (1964) 910.
60. M. Tümer, D. Ekinci, F. Tümer, A. Bulut, *Spectrochim. Acta, Part A: Mol. Biomol. Spectrosc.* 67 (2007) 916.
61. A. Patra, B. Sen, S. Sarkar, A. Pandey, E. Zangrando, P. Chattopadhyay, *Polyhedron* 51 (2013) 156.